Reactive and Functional Polymers 100 (2016) 18–25

Contents lists available at ScienceDirect

Reactive and Functional Polymers

journal homepage: www.elsevier.com/locate/react

Dendronization of chitosan films: Surface characterization and biological activity

A.A. Aldana [a], B. Barrios [b], M. Strumia [a], S. Correa [b], M. Martinelli [a,*]

[a] Instituto Multidisciplinario de Biología Vegetal (IMBIV), CONICET, Departamento de Química Orgánica, Facultad de Ciencias Químicas, Universidad Nacional de Córdoba, Haya de la Torre y Medina Allende, X5000HUA Córdoba, Argentina

[b] Centro de Investigaciones en Bioquímica Clínica e Inmunología (CIBICI-CONICET), Departamento de Bioquímica Clínica, Facultad de Ciencias Químicas, Universidad Nacional de Córdoba, Haya de la Torre y Medina Allende, X5000HUA Córdoba, Argentina

ARTICLE INFO

Article history:
Received 4 November 2015
Received in revised form 29 December 2015
Accepted 4 January 2016
Available online 6 January 2016

Keywords:
Biomaterials
Chitosan
Surface modification
Dendronization

ABSTRACT

An advanced modified chitosan film was designed and one-side-dendronized chitosan was obtained (ChPW). Undendronized chitosan films ChP and ChPW were characterized in terms of their chemical structure, morphology, and biological properties. Atomic force microscopy (AFM) and optical microscopy analysis were used to corroborate the topological changes of the modified dendronized side of the ChPW film. Both macrophages (RAW) and fibroblasts (NIH) were cultured and observed on three different extracellular matrices: ChP, ChPW, and cell culture plastic (control groups). ChP and ChPW showed noncytotoxicity toward RAW and NIH cells in contact with these films. The increased arginase activity with ChPW and ChP films suggests an alternative profile of L-arginine metabolism in RAW, which favors cell proliferation and wound healing. The results indicate that the ChPW scaffold is favorable for wound dressing in skin tissue engineering.

1. Introduction

Recently, the paradigm of biostable biomaterials has shifted to hydrolytic and enzymatic biodegradable biomaterials with medical and related applications [1].

In the coming years, many of the prosthetic devices used in temporary therapeutic applications to repair and regenerate damaged tissue will be replaced by biodegradable tools. The search for platform materials for the construction of biomaterials is the driving force behind novel areas of technology including tissue engineering, regenerative medicine, gene therapy, controlled drug delivery, and bionanotechnology [2–4].

The surface of the biomaterial is important as it is the point of contact with the biological environment [5]. An inadequate interaction between polymer and cells can trigger inflammation, infection, fibrosis, emboli, allergic thrombosis or implant encapsulation [6]. Dendronization is one of the surface modification techniques adopted with the aim of improving the biocompatibility, particularly the functionality of polymers used in tissue engineering. Dendrons have nanodimensions that can be immobilized on surfaces, leading to structural features within this size range. Modified nanostructured surfaces can be obtained with the ability to control the morphology and other surface properties of the dendrons such as wettability, roughness, chemical reactivity, and hardness. Dendronization of the surface of biomaterials can therefore be used to introduce specific properties for biomedical applications [7,8]. For instance, a significantly positive dendritic effect was observed in the antibody-binding capacity of immobilized bovine serum albumin (BSA) coupled to a dendronized support [9]. Benhabbour et al. found a significant increase in the affinity of epithelial cells for dendronized surfaces, with longer incubation times improving cell density on the surface. Our group has developed various dendronized materials to functionalize diverse substrates such as linear polymers and plane and curved inorganic surfaces that present new and specific properties. A prominent example of dendron as a mediator is the electrocatalytic oxidation of the nicotinamide adenine dinucleotide onto carbon electrodes [10]. The electrochemical properties are directly related to the number of electroactive functional groups incorporated into the dendritic molecule, a parameter which can be controlled [11].

The modification of natural polymers using dendritic structures is a particularly novel and interesting way of synthesizing highly functionalized and unconventional polysaccharide-based products of potential interest for different biomedical applications. Chitosan is a linear polymer of N-acetyl-D-glucosamine and a deacetylated glucosamine widely used as a wound-healing accelerator in clinical and veterinary medicine [12–14].

We used the dendronization process to obtain advanced chitosan microspheres and films whereby the resulting hybrids show improved mechanical properties and potential biological benefits [15,16]. Chitosan films dendronized on one side were prepared based on the reaction between a cross-linked biopolymer and dendron, conferring physical properties such as thermal stability, hydrophilic/hydrophobic balance, permeability, elastic modulus, and degree of swelling. These films

* Corresponding author at: Instituto Multidisciplinario de Biología Vegetal (IMBIV), CONICET, Departamento de Química Orgánica, Facultad de Ciencias Químicas, Universidad Nacional de Córdoba, Haya de la Torre y Medina Allende, X5000HUA, Córdoba, Argentina.
E-mail address: mmartinelli@fcq.unc.edu.ar (M. Martinelli).

http://dx.doi.org/10.1016/j.reactfunctpolym.2016.01.003
1381-5148/

have potential application as wound-dressing materials capable of maintaining a moist environment at the wound interface and acting as a barrier to microorganisms, removing excess exudate.

In order to fully assess the results obtained in these studies and reported by us, it is of fundamental importance to gain insight into the topology of the surface of the materials in question and evaluate the inflammatory response of the cells, thus opening a new array of chitosan-based scaffolds for use in biomedicine and, in particular, tissue engineering. We used different spectroscopic techniques to characterize topographical modification and assessed the L-arginine metabolism in macrophages and fibroblasts, the two key players in inflammatory response, to understand the effect of dendronized films on cells.

2. Experimental

2.1. Materials

Chitosan (Ch, 85% deacetylation (DA), LMW, Sigma-Aldrich); polyvinylpyrrolidone (P or PVP, Todo Droga); di-t-butyl-4-[2-(t-butoxycarbonyl)ethyl]-4-isocyanato-1,7-heptanedicarboxylate (W, Weisocyanate, Frontier Scientific Inc.); dibutyltin dilaurate (Sigma-Aldrich); dimethylacetamide (DMAc, Sintorgan); acetic acid glacial (Cicarelli); ninhydrin (Sigma-Aldrich); buffers (glycine, hydrochloric acid, potassium dibasic phosphate, and sodium hydroxide); and potassium bromide 99% Fourier transform infrared (FTIR) grade (Sigma-Aldrich) were used as received. Solvents were obtained from Sintorgan, purified by distillation, and dried. Lipopolysaccharide (LPS) was obtained from Sigma-Aldrich.

2.2. Instruments and techniques

FTIR and diffuse reflectance infrared Fourier transform (DRIFT) spectra were obtained on a Nicolet Avatar 360 FTIR spectrometer. Attenuated total reflectance Fourier transform infrared (ATR-FTIR) interferograms were acquired using the same spectrometer equipped with an attenuated Total Reflectance accessory. A 45 ZnSe crystal was used to monitor samples. All spectra were obtained with 32 scans at a 4.0 cm^{-1} resolution in a range between 4000 and 650 cm^{-1}. The thickness of ChP and ChPW was determined with Vernier Caliper 150 × 0.05 Mm/6 × 1/1000 Top Quality.

2.3. Preparation of films

As described in our previous report, the dendronized film was prepared by a two-step synthesis: chitosan film and one-side dendronization [16]. The chitosan film was obtained by the casting solvent method. Briefly, 1.00 g of chitosan was dissolved in 1.5% acetic acid solution (100 mL) and homogenized at room temperature overnight. PVP powder (0.180 g, 18% with respect to Ch) was subsequently added to the chitosan solution, and 50 mL of solution was cast on a glass plate (diameter 10 cm) and gradually dried in air at room temperature. The PVP chitosan films (ChP) were carefully removed from the Petri dishes, analyzed by ATR-FTIR spectroscopy, and characterized as previously described [16].

For dendronization, a special 25-mL nitrogen flask designed to hold a film in its base and equipped with a magnetic stirring bar was charged with a ChP film (0.100 g) in 10-mL DMAc. Weisocyanate (0.150 g, 0.15 mmol) and dibutyltin dilaurate (0.02 mL) were added and the mixture was stirred at 60 °C for 4 days. The film was washed with $CHCl_3$ to remove unreacted dendron, and dendronized chitosan films (ChPW) were carefully removed from the flask and dried under vacuum. The ChPW film was characterized by ATR-FTIR spectroscopy and the degree of dendronization was determined by the ninhydrin test [17].

2.4. Microscope techniques

2.4.1. Optic microscope and image analysis

Optic images of films were taken by a complementary metal-oxide semiconductor (CMOS) digital microscope. The images were digitalized in ImageJ 1.40 g® and analyzed after applying a gray scale and watershed transformation [18,19]. 3D graphics were subsequently obtained, with each point representing a spatial position (x and y coordinates) in pixels and width value (z-axis). The graphic profile was analyzed with the same program.

2.4.2. Atomic force microscopy

Atomic force microscopy (AFM) images of films were taken by ULTRAObjetive — Surface Imaging Systems GmbH microscopy (Nanoscopic Labs, INTI, Buenos Aires). The tapping mode, Si cantilevers with a constant nominal force at 48 N/m (Nanoprobes GmbH), and MPP-1123 Veeco tips were used. The screening speed was between 2 and 3 Hz. Starting height, breadth, and feedback were adjusted to obtain the best resolution. The images were taken at different points in each sample. The roughness analysis of each image was performed using Nanoscope 1.40® software. The root mean square (RMS) roughness (Rrms) was calculated by Nanoscope 1.40® software using the following equation:

$$\mathrm{RMS} = \sum_{i=1}^{N} \left[\frac{\left(z_i - \langle z \rangle^2 \right)}{N} \right]^{1/2}, \quad (1)$$

where z_i is the height of one point on the surface profile, ‹z› is the height of the surface profile, and *N* is the number of sampled points.

2.5. Ultraviolet–visible spectroscopy

Ultraviolet–visible (UV–Vis) spectra were obtained by UV–Vis Shimadzu 1800 spectrophotometer. The films were placed in a quartz cuvette and the spectra were registered between 200 and 700 nm. Air was used as background.

2.6. Macrophage and fibroblast culture with ChP and ChPW films

In order to evaluate the cellular response, 5-mm-diameter disks of ChPW and ChP films used as control were layered on 96-well plates. All samples were exposed to UV radiation for 15 min on each side for sterilization. The films were then washed exhaustively with complete RPMI (Roswell Park Memorial Institute) with 10% fetal bovine serum. After discarding the culture medium, macrophages (RAW 264.7 cells) and fibroblasts (NIH 3T3 cells) were seeded on each sample at a density of 1×10^5 cells/mL. Cells were stimulated with 1 μg/mL of LPS and cultured for 48 h with incubation in 5% CO_2 at 37 °C. Then, cell supernatants were collected to measure NO production and lactate dehydrogenase (LDH). The remaining supernatants were discarded and each well was rinsed thrice with phosphate buffer solution (PBS). Triton (0.1%, 50 μL) with 1% protease inhibitor was then added to each well and stirred for 30 min at room temperature. Cell lysate was used to determine arginase activity.

2.6.1. NO production

Nitrate was measured by the Griess reagent system (Promega, Madison, WI, USA) as described by Porporatto et al. [20] Briefly, 50 μL of cell-free culture supernatant was mixed with 50 μL of sulfanilamide solution (1% sulfanilamide in 5% phosphoric acid) and incubated for 5–10 min at room temperature, protected from light. Then, 50 μL of NED solution (0.1% N-1-napthylethylenediamine dihydrochloride in water) was dispensed to all wells and incubated at room temperature for 5–10 min, protected from light. Absorbance was measured within

30 min in a plate reader at 540 nm. Nitrite concentration was calculated with a sodium nitrite standard curve generated for each experiment. Three samples of each film type and control groups were tested. Data are presented as mean ± standard deviation (SD).

2.6.2. Arginase activity test

Arginase activity was measured as previously reported by Porporatto et al. [20] Briefly, 100 μL of cell lysate was mixed with 100 μL of 10 mM $MnCl_2$ in Tris–HCl 1 M, and the enzyme was activated for 10 min at 55 °C. Then, 25 μL of 0.5 M arginine (pH 9.7) was added to 25 μL of activated cell lysate, and the solution was incubated for 1 h at 37 °C. The enzymatic reaction was stopped with 400 μL of acid solution ($H_2SO_4/H_3PO_4/H_2O$) (1:3:7). Afterward, 25 μL of 9-wt.% α-isonitrosopropiophenone (dissolved in ethanol) was added to each vial and the mixture was heated at 100 °C for 1 h. After being cooled to room temperature, the absorbance at 540 nm was determined for urea content by a UV–Vis spectrophotometer. A urea calibration curve was plotted with increasing amounts of urea from 1.5 to 3 μg, using the procedure described earlier. One unit (U) of arginase activity was defined as the enzyme activity that catalyzes the production of 1 μmol of urea per minute under the condition of the assay.

2.6.3. LDH cytotoxicity assay

Reagent (LDH-P UV Wiener®) and sample were pre-incubated at 37 °C, and 3 mL of the reagent and 50 μL of the sample were added to a cuvette and mixed immediately. A stopwatch was simultaneously started. Initial absorbance was read after 30 s and then at 1, 2, and 3 min from the first reading. The average change in absorbance/min (ΔA/min) was calculated, subtracting each reading from the previous one and averaging the values. LDH activity was calculated by the following equation:

$$\mathrm{LDH} = \frac{\Delta Abs}{min} \times F, \tag{2}$$

where F (37 °C) is 8.095 (according to the manufacturer).

2.6.4. Adhesion test

ChP and ChPW film scaffolds were placed on 96-well culture plates, after which fibroblasts were seeded in each well at a density of 1×10^5 cells/mL. The cells were allowed to attach for 48 h at 37 °C in an atmosphere of 5% CO_2. In order to evaluate cell adhesion and proliferation on the substrates after 2 days of culture, the medium was aspirated and the attached cells were harvested using 0.25% trypsin–EDTA (ethylenediaminetetraacetic acid) solution and counted using a Neubauer hemocytometer. The nonattached cells were previously discarded by washing the cultures with PBS.

2.7. Statistical analysis

Data are shown as mean ± SD. The number of samples was three in each experiment. Differences between group means were assessed using one-way analysis of variance (ANOVA), followed by Student–Newman–Keuls tests for multiple comparisons. Statistical significance was set at $p < 0.05$.

3. Results and discussion

3.1. Preparation of dendronized chitosan films

Chemical modifications of chitosan were proposed to improve mechanical strength and chemical stability of the natural polymer in acidic media, thereby increasing its resistance to biochemical and microbiological degradation. A cross-linking step is required to reinforce the chemical stability of the biosorbents in acidic solution. We chose PVP as the cross-linker because of its biocompatibility [21]. Chitosan was mixed with PVP by blending, one of the most effective methods for acquiring new materials suitable for use in the field of biomedicine, and the film was made by casting. PVP is physically entangled in the chitosan network and the ninhydrin test showed a cross-linking degree of 93.7% [17].

Dendronization was carefully designed to modify one side of the cross-linked find [16], leaving the pristine chitosan on the opposite side. The dendronized chitosan film was successfully prepared by a covalent union with di-t-butyl-4-[2-(t-butoxycarbonyl)ethyl]-4-isocyanato-1,7-heptanedicarboxylate (Weisocyanate, W) dendron to yield ChPW film (Fig. 1). The degree of modification (8.67×10^{-5} mol/g of the film) was calculated by titration of the amino group (ninhydrin test), and the thickness of the film was found to be approximately 60–110 mm. ATR-FTIR analysis of the sample confirmed that dendronization occurred only on one surface of the film, where characteristic peaks of the dendron were observed, such as the *tert*-butyl methyl group at 850 and 756 cm^{-1} stretching and –CH–O–C ester group at 1225 and 2968 cm^{-1}. As the vibrations overlap, the band at 1729 cm^{-1} can be assigned to the C═O stretching of the dendron or urethane or urea bond formation. The characteristic bands of ChP showed no changes in the spectral profiles of the other side of the film [16].

The thickness of the ChP films before and after dendronization was similar (i.e., ~85 ± 15 μm). The instrument is not recognized enough to detect differences.

3.2. Microscope techniques

3.2.1. Optic microscope and image analysis

In order to evaluate topographic changes on the surface of the film, optic images on both sides of ChPW were recorded, analyzed, and compared with the image of undendronized film ChP (Fig. 2-I). The 3D surface graph (Fig. 2-II) was obtained by transforming the image: pixel distance and the darkness and brightness as low and high reflected light intensity. The black area in the image is a zone without film and the high reflected light intensity on each film is due to a defect in the program used for transforming 3D images

The optic images of both ChP and ChPW films (Fig. 2-I 1 and 2) are in gray scale and compare the modified [1] and nonmodified [2] sides of ChPW with nondendronized film.

In Fig. 2-II, the intensity of reflected light on the film of the dendronized side is significantly different from that of ChP and the nonmodified side of ChPW. Moreover, the nonmodified side of ChPW is similar to ChP (Fig. 2-II-1).

The cross-sectional graph is a transverse section of the 3D surface graph showing the roughness of the surface. Fig. 2-III-1 shows a difference in the roughness of the film surface between ChP (0–180 pixels) and ChPW (300–500 pixels).

It is important to highlight that the image shows a combination of topographic (surface roughness) and chemical (crystallinity and functional groups of material) effects [18,19], and it is clear that the dendron is present only on one side of the ChPW film. The process of dendronization yields a rough surface and increased light reflection, the latter most likely being due to one surface being more crystalline and the chemical nature of the incorporated molecule. The brighter (more crystalline) appearance indicates that the binding of dendrons to the film surface is orderly.

The image analysis of the ChP and ChPW (nonmodified side) surface films indicates similarities between the two, the results showing that dendronization modifies only one face of the ChPW film.

3.2.2. Atomic force microscopy

AFM is a useful tool for obtaining information of the surface characteristics of films. The AFM images of ChP and ChPW are presented in Fig. 3

The surface of ChP is smoother than that of ChPW, the bright dots on the latter indicating raised areas forming a rough surface. The clusters of

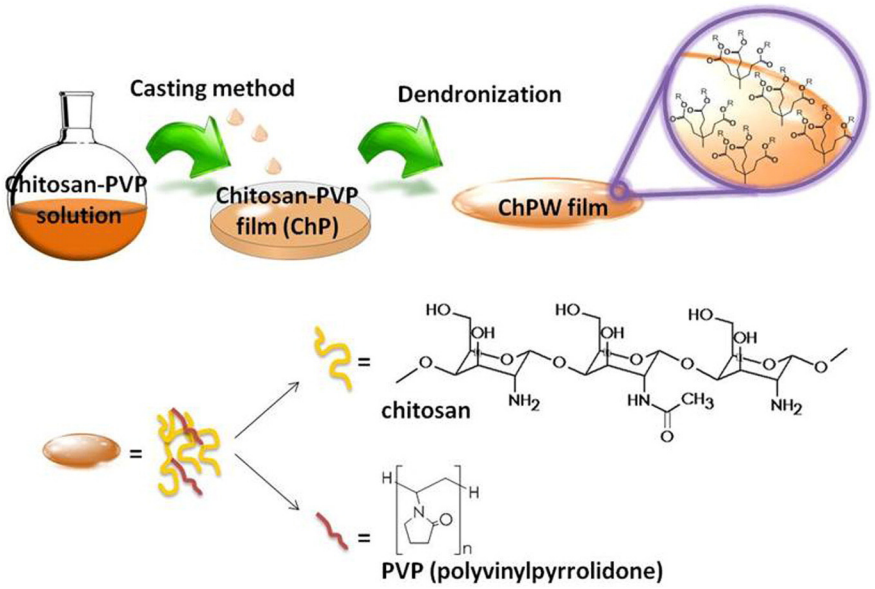

Fig. 1. Scheme of dendronization of chitosan.

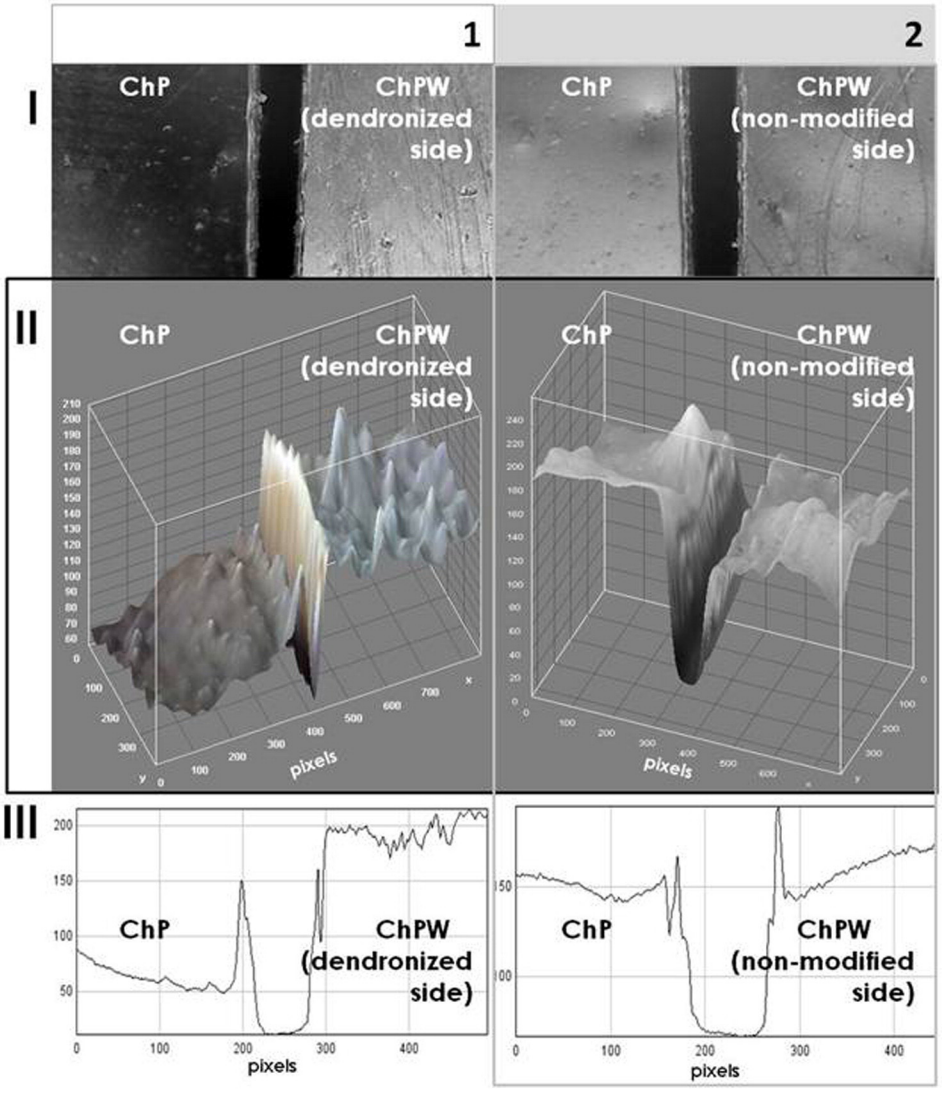

Fig. 2. Optic images (I) of films and their 3D surface (II) and cross-section (III) analysis comparing non-dendronized film (ChP) with: 1 — modified side of ChPW and 2 — non-modified side of ChPW.

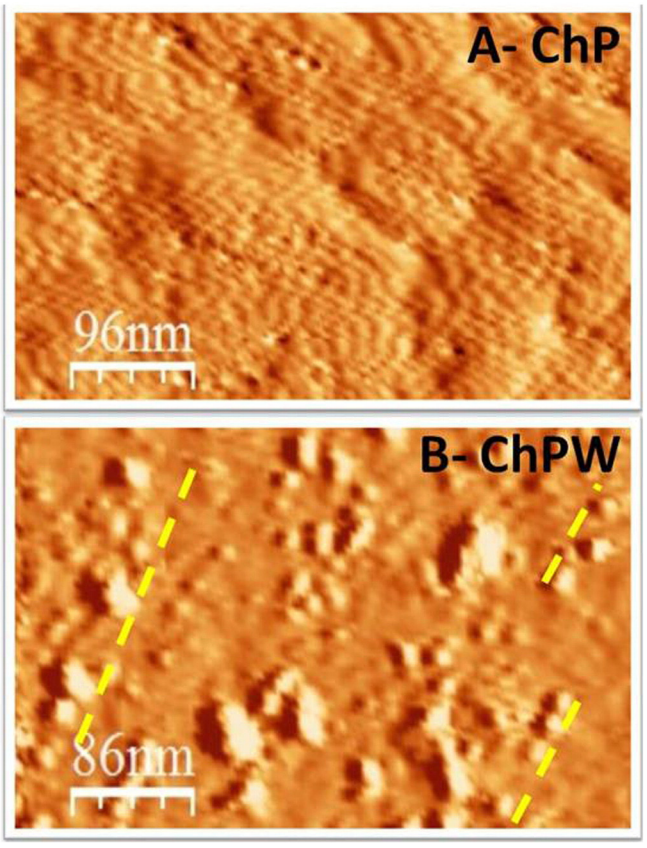

Fig. 3. AFM images: ChP (A) and ChPW (B).

spots on the surface present a certain order, as indicated by the yellow lines in Fig. 3.

The organization of dendrons and dendrimers on different supports (organic and inorganic) is controlled by the stiffness, chemical structure, steric interactions, shape, and size of the dendritic structures [22], and it was based on this concept that the idea of binding W organized into clusters aligned on one side of the films arose.

The roughness index, a statistical value obtained from the height profile registry to determine surface irregularities, was used to analyze the surface roughness. The values obtained were 0.52 and 5.84 for the ChP and ChPW (dendronized side), respectively, indicating that the difference in roughness is due to the attachment of the dendrons to the film, the high points observed on the surface of ChPW corresponding to the formation of small clusters of W.

The topological effect of dendronization and its organization on the surface of the film were evaluated by means of nano- and micrometer microscopy studies. The optical microscopy analysis determined the difference between the unmodified and modified faces of the ChPW film. The ordering of the dendritic structures determined by AFM is correlated with the reflective surface observed by optical microscopy.

3.3. UV–Vis spectroscopy

UV–Vis spectra of ChP and ChPW were taken. In order to facilitate comparison and analysis of the data, the absorbance was normalized to the film thickness (Fig. 4).

The presence of the dendron on the matrix increases the absorbance of the band, shifting it to a shorter wavelength – the so-called hypsochromic shift – because of the presence of new functional groups. The ChPW film has the dendron ester groups and urethane and urea corresponding to the binding of the isocyanate group (dendron) with the amino group and hydroxyl Ch, respectively.

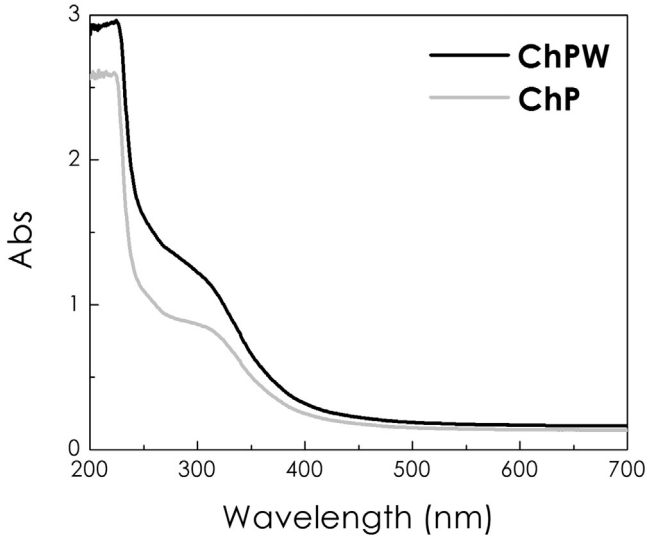

Fig. 4. UV–visible spectrum of ChP and ChPW films.

The results of the spectroscopic analysis indicate that the ChPW film allows lesser light through it than the ChP film, so that the interaction of ChPW with the UV–Vis light is of a higher order than in the case of the film without dendron. This difference in the interaction with light in the presence of the dendron (Fig. 4) was also observed in optic microscope studies.

3.4. Macrophage and fibroblast culture with ChP and ChPW films

Fibroblasts have the ability to migrate to the injured site, proliferate, and produce the extracellular matrix components. These processes are stimulated and regulated by cytokines and growth factors.

Macrophages are essential for wound healing. These cells show varying degrees of functional activation in homeostatic and pathological conditions [23]. The two ends of the spectrum of the activation of macrophages have been called “classic o” (M1), and “alternate” (M2) [24], and they play opposing roles in the immune and inflammatory response [25]. The profile of macrophage activation is linked with the metabolic pathway of arginine, which may be mediated by the induced form of nitric oxide synthase (iNOS) or arginase. In M2 macrophages, the activation of the arginase pathway produces urea and ornithine, which stimulate collagen production and cell proliferation [26]. In M1 cells, arginine metabolism is shifted to NO and citrulline, which is toxic to microbes and parasites and also antiproliferative [20]. Therefore, tests with macrophages (RAW) and fibroblasts (NIH) were performed to assess whether contact with the ChP and ChPW promotes polarization.

3.4.1. Determination of L-arginine metabolism

The effect of ChP and ChPW films on L-arginine metabolism of macrophages (RAW cells) and fibroblasts (NIH 3T3 cells) was evaluated. The arginase activity of unstimulated macrophages (basal) did not statistically differ between control and ChP or ChPW film cultures. Upon the addition of LPS – a stimulus of L-arginine metabolism via iNOS – to macrophages, these values were not statistically modified in cells in contact with films. On the contrary, the LPS stimulus increased NO production in control cultures, as LPS induces an iNOS pathway. However, there were no differences between basal and LPS-stimulated film cultures (gray bars in Fig. 5). In macrophage cultures in contact with the films, NO release was approximately 40% lower than that in the controls, suggesting an attenuated inflammatory profile in macrophages

In fibroblasts, the two metabolic pathways were not affected by the films (Fig. 6). NO release was not stimulated by LPS, and therefore control cells with or without stimulus showed similar levels of NO production. When the cells are in contact with the films, arginase activity

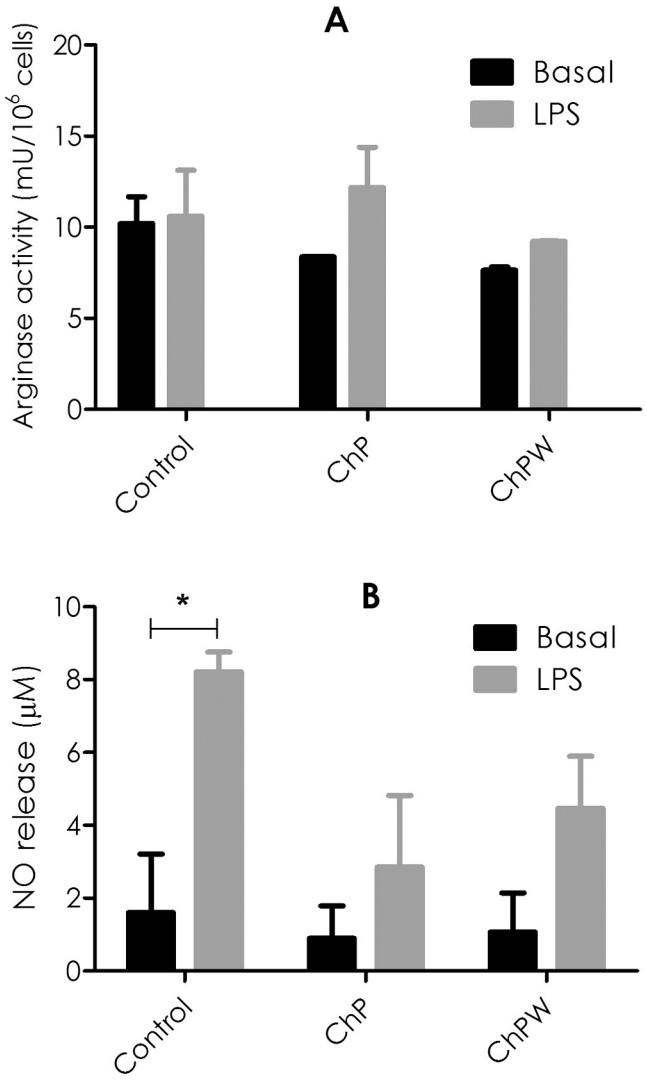

Fig. 5. A — Arginase activity levels and B — amount of nitric oxide-released macrophages in contact or not (control) with ChP or ChPW films, without stimuli (basal ■) or with stimuli (LPS ■).

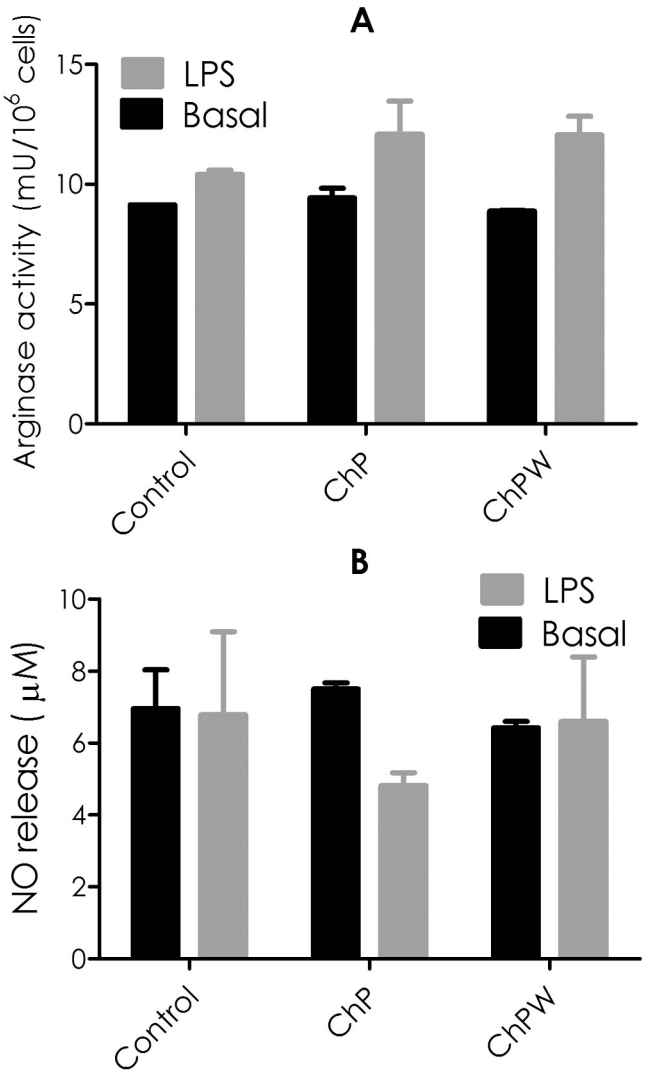

Fig. 6. A — Arginase activity levels and B — amount of nitric oxide-released fibroblasts in contact or not (control) with ChP or ChPW films, without stimuli (basal ■) or with stimuli (LPS ■).

increases slightly with LPS stimulus. These results demonstrate the resting status of fibroblasts when in contact with ChP and ChPW films. It is important to highlight that in vitro assays of both RAW and NIH cell lines did not show an inflammatory profile. In addition, iNOS activity decreases and arginase activity increases in the macrophages, suggesting the activation of an alternative profile that brings on cell proliferation and hence healing of the wound while the fibroblasts seem less primed.

3.4.2. LDH cytotoxicity assay

LDH is an intracellular enzyme whose release indicates damage to the plasmatic membrane. Fig. 7-A and B shows LDH levels in NIH and RAW cells, respectively. For fibroblasts, the films tend to slightly increase LDH values, indicating cell death. However, LDH levels for macrophages in contact with films are the same as those for controls, indicating that ChP and ChPW films are biocompatible with macrophages.

3.4.3. Adhesion test

Adhesion test was carried out on fibroblasts as these cells showed a slight increase in cell death after contact with films.

Earlier, hydrophilicity/hydrophobicity of film surface was evaluated by contact angle, swelling index, and water vapor permeability measures [16]. The equilibrium swelling of the film was studied at different pH values for 7 h, and they were not degraded. According to the values of contact angle (111.5°) and water vapor permeability, after dendronization, the films were found to be more hydrophobic. In view of this context, it is considered that the dendronization process would affect adherence of cells to the side of the film that is dendronized.

As observed in Fig. 8, the majority of adhered cells were on ChP films; it is likely that the roughness and chemical features of dendronized films had an effect on cell adhesion. Corrales et al. [6] studied the cell adhesion of polycaprolactone (PCL) matrices and clay compared with commercial control films. They observed that cell adhesion increases with time (1, 4, and 6 days), being the maximum adherence of two cells per film unit (4 mm of diameter). The ChP and ChPW films showed better results than PCL matrices and clay films in terms of cell adhesion, as the area used for the adhesion test with PCL and clay films was approximately six times larger. ChP and ChPW could therefore be appropriate biomaterials for use in tissue engineering, particularly as wound dressings.

4. Conclusions

Chitosan films were obtained by a simple and efficient technique, and dendronization of one face of the film was successfully achieved, generating topographic and chemical changes on the dendronized

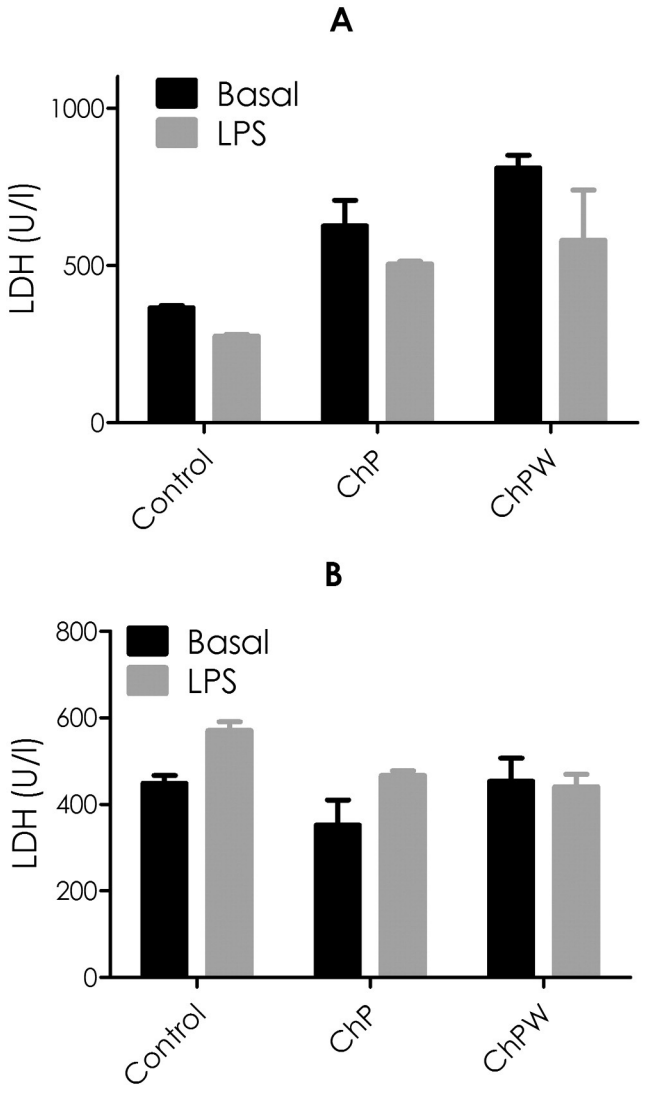

Fig. 7. LDH levels in fibroblast (A) or macrophages (B) in contact or not (control) with ChP or ChPW films, without stimuli (basal ■) or with stimuli (LPS ■).

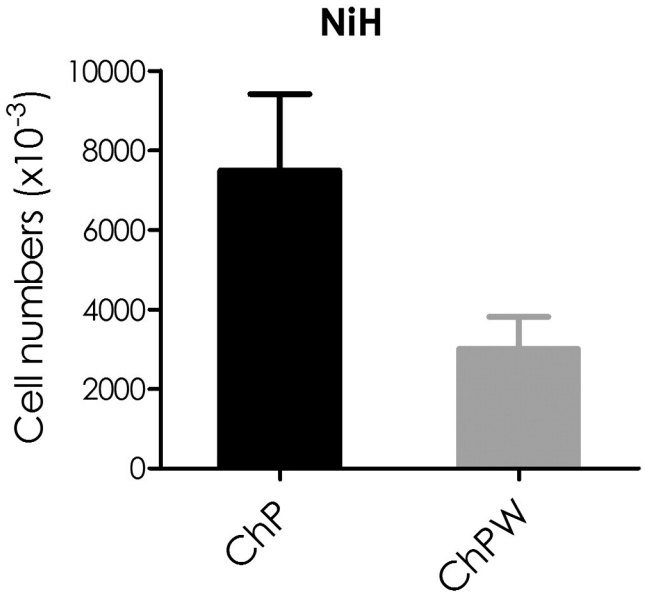

Fig. 8. Number of fibroblast cells on ChP and ChPW films as evaluated during the adhesion assay.

surface. AFM and scanning electron microscopy were used to corroborate the topographic changes. The dendrons were placed on aligned agglomerates over one face of ChPW film.

The ChP and ChPW films did not stimulate or enhance an inflammatory profile in fibroblasts and macrophages cultured for 48 h. Furthermore, the films were able to activate an alternative profile of L-arginine metabolism in macrophages, which enhance cell proliferation and wound healing.

The plasmatic membrane of macrophages was not affected by contact with ChP and ChPW, suggesting that the films are biocompatible with macrophages.

The microbiological properties and antibacterial capacity of these films are highly relevant to their application in tissue engineering and regenerative medicine [16].

ChPW could be used as a wound dressing by exposing the dendronized face to air and placing the other face in contact with the wound. The hydrophilic face permits a higher water absorption and bacterial inhibition [16] and the ChP face has good adherence to cells.

Acknowledgments

The authors gratefully acknowledge the financial assistance of FONCYT, CONICET, and SECYT of the UNC in Argentina. Aldana A.A. thanks CONICET for the fellowship awarded. The authors also thank Dr. Marcelo Romero for optical microscopy measurements.

References

[1] T. Maharana, S. Pattanaik, A. Routaray, N. Nath, A.K. Sutar, Synthesis and characterization of poly(lactic acid) based graft copolymers, React. Funct. Polym. 93 (2015) 47–67.
[2] L.S. Nair, C.T. Laurencin, Biodegradable polymers as biomaterials, Prog. Polym. Sci. 32 (2007) 762–798.
[3] N.E. Valderruten, J.D. Valverde, F. Zuluaga, E. Ruiz-Durántez, Synthesis and characterization of chitosan hydrogels cross-linked with dicarboxylic acids, React. Funct. Polym. 84 (2014) 21–28.
[4] F. Tasselli, A. Mirmohseni, M.S. Seyed Dorraji, A. Figoli, Mechanical, swelling and adsorptive properties of dry–wet spun chitosan hollow fibers crosslinked with glutaraldehyde, React. Funct. Polym. 73 (2013) 218–223.
[5] X. Zhu, H. Wu, J. Yang, J. Tong, J. Yi, Z. Hu, J. Hu, T. Wang, L. Fan, Antibacterial activity of chitosan grafting nisin: preparation and characterization, React. Funct. Polym. 91–92 (2015) 71–76.
[6] T. Corrales, I. Larraza, F. Catalina, T. Portolés, C. Ramírez-Santillán, M. Matesanz, C. Abrusci, In vitro biocompatibility and antimicrobial activity of poly(ε-caprolactone)/montmorillonite nanocomposites, Biomacromolecules 121128090442006 (2012).
[7] C.C. Lee, M. Yoshida, J.M.J. Frechet, E.E. Dy, F.C. Szoka, In vitro and in vivo evaluation of hydrophilic dendronized linear polymers, Bioconjug. Chem. 16 (2005) 535–541.
[8] H. Frauenrath, Dendronized polymers—building a new bridge from molecules to nanoscopic objects, Prog. Polym. Sci. 30 (2005) 325–384.
[9] S.R. Benhabbour, H. Sheardown, A. Adronov, Cell adhesion and proliferation on hydrophilic dendritically modified surfaces, Biomaterials 29 (2008) 4177–4186.
[10] J.I. Paez, M.C. Strumia, M.C.G. Passeggi Jr., J. Ferrón, A.M. Baruzzi, V. Brunetti, Spontaneous adsorption of 3,5-bis(3,5-dinitrobenzoylamino) benzoic acid onto carbon, Electrochim. Acta 54 (2009) 4192–4197.
[11] F.E. Appoh, H.-B. Kraatz, Voltammetric studies of dendrimer multilayers: layer-by-layer assembly of metal-peptide dendrimers multilayers, J. Appl. Polym. Sci. 111 (2009) 709–723.
[12] R. Jayakumar, D. Menon, K. Manzoor, S.V. Nair, H. Tamura, Biomedical applications of chitin and chitosan based nanomaterials—a short review, Carbohydr. Polym. 82 (2010) 227–232.
[13] H. Ueno, T. Mori, T. Fujinaga, Topical formulations and wound healing applications of chitosan, Adv. Drug Deliv. Rev. 52 (2001) 105–115.
[14] R.A.A. Muzzarelli, Chitins and chitosans for the repair of wounded skin, nerve, cartilage and bone, Carbohydr. Polym. 76 (2009) 167–182.
[15] A.A. Aldana, M.C. Strumia, M. Martinelli, The cooperative effect in dendronized chitosan microbeads, Aust. J. Chem. (2015).
[16] A.A. Aldana, R. Toselli, M.C. Strumia, M. Martinelli, Chitosan films modified selectively on one side with dendritic molecules, J. Mater. Chem. 22 (2012) 22670.
[17] M.M. Leane, R. Nankervis, A. Smith, L. Illum, Use of the ninhydrin assay to measure the release of chitosan from oral solid dosage forms, Int. J. Pharm. 271 (2004) 241–249.
[18] H. Zhou, J. Wu, J. Zhang, Digital image processing, in: J.W.H. Zhou, J. Zhang, Ventus Publishing ApS (Eds.),Part I, BookBoon, 2010.
[19] H. Zhou, J. Wu, J. Zhang, Digital image processing, in: J.W.H. Zhou, J. Zhang, Ventus Publishing ApS (Eds.),Part II, BookBoon, 2010.

[20] C. Porporatto, I.D. Bianco, C.M. Riera, S.G. Correa, Chitosan induces different L-arginine metabolic pathways in resting and inflammatory macrophages, Biochem. Biophys. Res. Commun. 304 (2003) 266–272.
[21] W. Wang, A. Wang, Synthesis and swelling properties of pH-sensitive semi-IPN superabsorbent hydrogels based on sodium alginate-g-poly(sodium acrylate) and polyvinylpyrrolidone, Carbohydr. Polym. 80 (2010) 1028–1036.
[22] J.I. Paez, M. Martinelli, V. Brunetti, M.C. Strumia, Dendronization: a useful synthetic strategy to prepare multifunctional materials, Polymers 4 (2012) 355–395.
[23] S. Gordon, P.R. Taylor, Monocyte and macrophage heterogeneity, Nat. Rev. Immunol. 5 (2005) 953–964.
[24] S. Gordon, Alternative activation of macrophages, Nat. Rev. Immunol. 3 (2003) 23–35.
[25] A. Puig-Kröger, E. Sierra-Filardi, A. Domínguez-Soto, R. Samaniego, M.T. Corcuera, F. Gómez-Aguado, M. Ratnam, P. Sánchez-Mateos, A.L. Corbí, Folate receptor β is expressed by tumor-associated macrophages and constitutes a marker for M2 anti-inflammatory/regulatory macrophages, Cancer Res. 69 (2009) 9395–9403.
[26] A.E. Ulland, J.D. Shearer, C. Coulter, M.D. Caldwell, Altered wound arginine metabolism by corticosterone and retinoic acid, J. Surg. Res. 70 (1997) 84–88.